

Modeling and Analysis of Composite Antenna Superstrates Consisting on Grids of Loaded Wires

Pekka M. T. Ikonen, *Student Member, IEEE*, Elena Saenz, *Student Member, IEEE*,
Ramón Gonzalo, *Member, IEEE*, and Sergei A. Tretyakov, *Senior Member, IEEE*

Abstract— We study systematically the characteristics of antenna superstrates based on closely located periodical grids of loaded wires. An explicit method based on the local field approach is used to study the reflection and transmission properties of such superstrates. It is shown that as a result of proper impedance loading there exists a rather wide frequency band over which currents induced to the grids cancel each other leading to a wide transmission maximum. In this regime radiation is produced by the magnetic dipole moments created by circulating out-of-phase currents flowing in the grids. An impedance matrix representation and equivalent circuit model are derived for the superstrates, and the analytical results are validated using full wave simulations. As a practical application we study the radiation pattern of a dipole antenna illuminating finite size superstrates. Discussion is conducted on the effects of finite structural dimensions and feed structures.

Index Terms— Superstrate, wire grid, capacitively loaded wire, local field, gain enhancement

I. INTRODUCTION

Artificial dielectrics, implemented e.g. as arrays of wires, have been used for decades as light-weight beam shaping elements, see e.g. [1]–[6] for some early contributions and [7], [8] for some more recent results. It is nowadays well understood that some electromagnetic (photonic) crystals simulate the behavior of homogeneous materials with ultra-low refractive index near stop-band edges [9], [10], [11]. This observation has led to several studies concerning directive antenna design using such periodical structures to shape the beam of a low-gain primary radiator, e.g. [12]–[14]. It is also known that a slight local change in the period of electromagnetic crystals leads to localized resonant modes which can be used for the realization of devices radiating energy in a very narrow angular range [15]. Typically, radiating sources are placed inside Fabry-Perot resonant cavities formed by removal of rows of wires or dielectric rods in a periodical lattice [16]–[21]. The long-known ideas of creating resonant cavities using partially reflecting sheets [22] have also been widely employed in recent gain enhancement designs [23]–[27]. Similarly, frequency-selective surfaces on top of ground planes have been used to implement Fabry-Perot resonant cavities, e.g. [28]. Antenna superstrates are another well-known gain enhancement tool [29], [30]. As in the case of

defected electromagnetic crystal structures [16]–[21] one of the key ideas of different superstrates is to allow radiation from a primary source to spread over a larger radiating aperture. Recently, very exotic structures such as material covers or superstrates aimed to possess double-negative behavior [31] have been proposed for this purpose [32], [33], [34].

The goal of this work is to present an analytical methodology for studying the characteristics of a class of composite structures proposed as superstrates for low-gain antennas. More precisely, we consider two closely located parallel grids of capacitively loaded wires having possibly a grid of continuous (purely inductive) wires between them. The methodology presented here can, however, be extended to study the characteristics of other kinds of superstrates based on multiple grids of wires loaded with arbitrary distributed impedance. The physics behind the operational principle of such superstrates is clarified. We will also briefly discuss extending the methodology to handle strongly coupled dipole grids, as over a certain frequency range the dispersion properties of a capacitively loaded wire medium are known to resemble those of a medium consisting of small dipole scatterers [35]. The transmission properties of strongly coupled dipole grids have in the past been analyzed with an application to frequency-selective surfaces or electromagnetic band-gap structures e.g. in [36], [37], [38]. In these works the response has been calculated using an iterative method based upon solving a set of coupled integral equations for the unknown element currents and aperture fields. The method presented here is explicit, and despite taking into account all the near field interactions between the grids (higher order Floquet modes) it remains computationally efficient and physically illustrative.

The novelty of the proposed superstrate designs is to excite resonant oscillations in capacitively loaded wires (this way creating a wider radiating aperture) while maintaining partial transparency of the structure. In the designs considered here the source field induces out-of-phase currents to the loaded wire pairs, and the pairing currents give rise to magnetic dipole moments that produce radiation. We start the analysis by explaining heuristically the operational principle of the superstrates. After this, the local field method is used to analytically study the reflection and transmission properties of the superstrates. The results are validated using full wave simulations and we also calculate the electric and magnetic dipole moments induced to one of the structures. It is shown that a strong resonant enhancement of the superstrate aperture field can be achieved with very thin superstrates and without

P. M. T. Ikonen and S. A. Tretyakov are with the Radio Laboratory / SMARAD Centre of Excellence, Helsinki University of Technology, P.O. Box 3000, FI-02015 TKK, Finland. (e-mail: pekka.ikonen@tkk.fi). E. Saenz and R. Gonzalo are with the Department of Electrical and Electronic Engineering, Public University of Navarra, Campus Arrosadia E-31006, Pamplona-Navarra, Spain.

the need to create resonant cavities. Based on the electrodynamic model an impedance matrix representation is derived for the superstrates in order to construct an equivalent circuit model taking into account the mutual interaction between the wire grids. Finally, we calculate and simulate some example radiation patterns of dipole antennas illuminating finite size superstrates. It is demonstrated that the key features observed with plane wave excitation of infinite superstrates are also seen with finite size superstrates illuminated by dipole antennas. The effects of finite structural sizes to the superstrate performance are discussed.

II. HEURISTIC OPERATIONAL PRINCIPLE

The superstrate studied in this work is schematically depicted in Fig. 1a. The first and third grids (see the numbering of grids in Fig. 1a) consist of parallel capacitively loaded¹ wires, while the second grid consists of continuous (inductive) thin wires. Please note that in Fig. 1 round wires have been replaced by strips to reflect one feasible implementation technique. However, in the following analytical derivation we assume round wires since electrically thin wires and strips behave in a similar manner. To account for the difference in the geometry an effective radius of wires is introduced in the analytical analysis.

The properly designed structure is expected to show an analogy with double-negative behavior: In a certain frequency range the metal strips constituting a capacitively loaded wire can be interpreted as short dipoles, and every pair of such dipoles (sitting in grids 1 and 3) shows a magnetic resonant mode which can be utilized to create a response similar to that of split rings [39], [40]. On the other hand, the long conductors provide plasma-like electric response as in wire media [41], [42]. Recently, it has been reported that only short

¹In this work capacitive loading is created by cutting the wires.

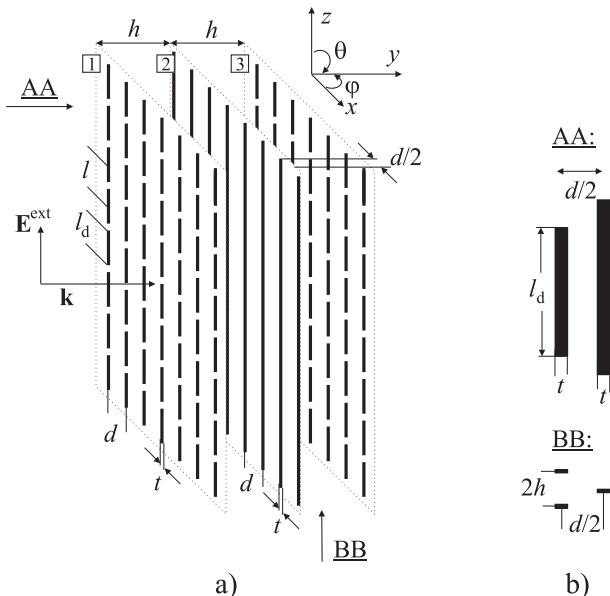


Fig. 1. a) A schematic illustration of the proposed superstrate (not necessarily in scale). b) Unit cell geometry.

wire pairs are enough to obtain double-negative behavior [43], [44]. For describing the radiation properties of the superstrate we concentrate, however, on the local dipole moments induced in the structure.

Consider first only a pair of two capacitively loaded wires (we assume that grid 2 is absent). At a certain frequency the currents induced to individual pairing metal strips cancel each other allowing the incident wave to propagate through the grids. To widen the pass-band one can bring a grid of solid wires in between the loaded wire grids. In this case two modes appear due to the capacitances and mutual coupling between the loaded wires and the continuous wires. In other words, there are now two possibilities for the currents in the grids to cancel each other, and by properly choosing the unit cell dimensions both transmission bands can be merged together. Since the superstrate is *volumetric* (though the total thickness $2h$ is in practise extremely small compared with the wavelength) the cancelation of total electric current does not mean the cancelation of radiation: The superstrate is effectively transparent for the incident waves, however, the magnetic dipole moments induced in the pairing metal strips produce radiation. These dipole moments are distributed over the superstrate, thus every strip pair in the structure will radiate principally in a similar manner allowing the realization of a more or less uniform aperture phase distribution on the outer superstrate surface.

Another important practical issue, discussed later in more details, is the interaction between a closely located primary radiator and the loaded wire grids. It will be shown that in case of capacitively loaded wires the source can be brought very close to the grids without deteriorating the radiation resistance. This allows to design low-profile and effectively radiating structures.

III. LOCAL FIELD METHOD TO STUDY THE SUPERSTRATE PROPERTIES

A. Plane-wave reflection and transmission coefficients and induced electric and magnetic dipole moments

Though in most of the following parts of the paper we consider the situation when only the grids of loaded wires are present, we will conduct the derivation for the three-grid structure depicted in Fig. 1a. This is to illustrate the feasibility of our method to handle inclusions with different polarizabilities. At this point we assume that the grids in the superstrate are infinite in z and x directions. Moreover, the transversal thickness t of the inclusions (equivalently the radius r_0 of round wires) is small compared to the wavelength. We assume the normal plane-wave incidence (though the analysis can be carried out for oblique incidence as well) and write the external electric field as

$$\mathbf{E}^{\text{ext}} = \mathbf{u}_z E^{\text{ext}} e^{-jk_y y}. \quad (1)$$

We write down the equation for the local electric field acting on the surface of a reference element in each of the grids. Consider first the unloaded reference wire. We assume that the wires are thin enough so that we can represent them as infinitely long current lines located at the wires axis. The

relation between the amplitude of the local electric field E_z^{loc} acting on the wire surface and current I flowing on the wire surface reads

$$E_z^{\text{loc}} = \alpha_0^{-1} I, \quad (2)$$

where α_0 is the susceptibility of the wire which can be determined from the boundary condition on the wire surface (see e.g. [45]):

$$\alpha_0 = \left[\frac{\eta(k^2 - k_z^2)}{4k} H_0^{(2)} \left(\sqrt{k^2 - k_z^2} r_0 \right) \right]^{-1}, \quad (3)$$

where η is the wave impedance in the matrix material (host material for the wires), k_z is the z -component of the wave vector, and $H_0^{(2)}$ represents the Hankel function of the second kind and zero order. If the wires are loaded with a certain uniformly distributed impedance per unit length Z , the inverse of the wire susceptibility becomes [35], [46]:

$$\alpha^{-1} = \alpha_0^{-1} + \frac{k^2 - k_z^2}{k^2} Z. \quad (4)$$

The amplitude of the local electric field acting on the reference wires can also be expressed in the following manner:

$$\alpha^{-1} I_1 = E^{\text{ext}} + \beta(0) I_1 + \beta(h) I_2 + \beta(2h) I_3, \quad (5)$$

$$\alpha_0^{-1} I_2 = E^{\text{ext}} e^{-jkh} + \beta(h) I_1 + \beta(0) I_2 + \beta(h) I_3, \quad (6)$$

$$\alpha^{-1} I_3 = E^{\text{ext}} e^{-j2kh} + \beta(2h) I_1 + \beta(h) I_2 + \beta(0) I_3, \quad (7)$$

where $\beta(0)$ is so called self interaction coefficient (eq. (11) in [41], see also [47]):

$$\begin{aligned} \beta(0) = & -\frac{\eta(k^2 - k_z^2)}{2k} \left[\frac{1}{d\sqrt{k^2 - k_x^2 - k_z^2}} - \frac{1}{2} \right. \\ & \left. + \frac{j}{\pi} \left(\log \frac{d\sqrt{k^2 - k_z^2}}{4\pi} + \gamma \right) \right. \\ & \left. + \frac{j}{d} \sum_{n \neq 0} \left(\frac{1}{\sqrt{(k_x + 2\pi n/d)^2 + k_z^2 - k^2}} - \frac{d}{2\pi|n|} \right) \right], \quad (8) \end{aligned}$$

and $\beta(h)$, $\beta(2h)$ are mutual interaction coefficients (eqs. (12) and (13) in [41]):

$$\beta(ih) = -\frac{\eta(k^2 - k_z^2)}{2kd} \sum_{n=-\infty}^{n=+\infty} \frac{e^{-jk_x^{(n)} ih}}{k_x^{(n)}}, \quad i = 1, 2. \quad (9)$$

Above $\gamma \approx 0.5772$ is the Euler constant, and $k_x^{(n)}$ is the z -component of the n -th Floquet mode wave vector [41]:

$$k_x^{(n)} = -j\sqrt{(k_x + 2\pi n/d)^2 + k_z^2 - k^2}, \quad \text{Re}\{\sqrt{\cdot}\} > 0. \quad (10)$$

Physically $\beta(0)$ tells how strongly the wires located in the same grid as the reference wire influence the local field, whereas $\beta(h)$, $\beta(2h)$ measure the influence of the other two grids. Now we can cast eqs. (5)–(7) in the following form:

$$\begin{aligned} -E^{\text{ext}} \begin{pmatrix} 1 \\ e^{-jkh} \\ e^{-j2kh} \end{pmatrix} = \\ \begin{pmatrix} \beta(0) - \alpha^{-1} & \beta(h) & \beta(2h) \\ \beta(h) & \beta(0) - \alpha_0^{-1} & \beta(h) \\ \beta(2h) & \beta(h) & \beta(0) - \alpha^{-1} \end{pmatrix} \begin{pmatrix} I_1 \\ I_2 \\ I_3 \end{pmatrix}. \quad (11) \end{aligned}$$

From the above equation currents in different grids can be solved by simple inversion. The averaged current density induced to the grids is defined as

$$\widehat{J}_i = \frac{I_i}{d}, \quad i = 1, 2, 3. \quad (12)$$

In the far zone, the reflected field of one grid in the normal direction is a plane-wave field, and close to the grids this plane-wave field can be expressed as [46]

$$E_i^{\text{sc}} = -\frac{\eta}{2} \widehat{J}_i. \quad (13)$$

After this we can calculate the total reflection and transmission coefficients. The reflection and transmission coefficients referred to the plane of the first grid read:

$$R = \frac{\sum_{i=1}^3 E_i^{\text{sc}} e^{-jkh(i-1)}}{E^{\text{ext}}}, \quad (14)$$

$$T = 1 + \frac{\sum_{i=1}^3 E_i^{\text{sc}} e^{jkh(i-1)}}{E^{\text{ext}}}. \quad (15)$$

As an example, we calculate the dipole moments induced to a structure that consists of two grids of capacitively loaded wires (in this case grid 2 is absent in Fig. 1a). The electric and magnetic dipole moment densities on the superstrate are calculated as [48]

$$\mathbf{p} = \int \mathbf{u} \rho \, dV, \quad (16)$$

$$\mathbf{m} = \mu_0 \int \mathbf{r} \times \mathbf{J} \, dV, \quad (17)$$

where ρ is the charge density in the unit volume (see Fig. 1b for the unit cell) and \mathbf{J} is the corresponding volumetric current density. When the integrations are conducted in our geometry the dipole moments take the following form:

$$p = \frac{l_d}{j\omega} (I_1 + I_3), \quad (18)$$

$$m = \mu_0 \frac{hl_d}{2} (I_1 - I_3). \quad (19)$$

1) Discussion on the modeling approach: It is known that at low frequencies (frequencies at which the structural dimensions are small compared to the wavelength) the dispersion properties of lattices of capacitively loaded wires and dipole scatterers rather closely resemble each other [35]. Noticeable deviation is seen only close to the frequencies where the strip length in the loaded wires becomes resonant. At these frequencies (and at higher frequencies), for accurate analysis, one should model the first and third grids as grids of dipole scatterers. The principal ideas of the above derivation would still be the same, however, different models for inclusion polarizabilities and interaction constants should be used [49]–[51]. It will be demonstrated below, however, that in the frequency regime where the superstrates are feasible for antenna beam shapers, the capacitively loaded wire model leads to accurate results. It is also important to note that the method described above can be used to study the properties of superstrates formed by an arbitrary number of grids, and the distributed impedance loading the wires can be arbitrary.

2) *Numerical validation.* For the validation of the analytical method we choose for the superstrate the structural parameters considered in [34] (the notation is clear from Fig. 1): $l = 12.11$ mm, $l_d = 10.11$ mm, $t = 1$ mm, $d = 4.8$ mm, $h = 1$ mm. We conduct strip to wire conversion and use text book formulas to estimate the distributed capacitance due to the slits in the wires in first and third grids.

For calculating the reflection and transmission coefficients we consider separately two structures. In the first one only the two grids of capacitively loaded wires are present. In the second case we bring the grid of continuous wires in between the loaded wire grids as shown in Fig. 1a. Reflection and transmission coefficients are calculated using eqs. (14) and (15). We also simulate the coefficients using Ansoft HFSS [52] (the unit cell for HFSS simulations is shown in Fig. 1b). The results of calculations and simulations are depicted in Figs. 2 and 3. We observe that the agreement between the analytical calculations and simulations is good up to 13 GHz. At this frequency the length of the metal strips in the loaded wires is already roughly $\lambda/2$, so it is clear that at frequencies higher than 13 GHz (in this particular case) the local field model based on loaded wires fails. Nevertheless, for antenna applications we are interested in the frequency regime where the superstrates are partially transparent (frequency regime in which the transmission maxima lie, see Figs. 2, 3), and at these frequencies the analytical model works well.

The amplitudes of electric and magnetic dipole moment densities induced to the superstrate consisting of the two grids of loaded wires are shown in Fig. 4. As speculated earlier, the magnetic dipole moment shows a strong resonance in the vicinity of the frequency where the structure is effectively transparent for incident radiation. It is worth to note that at the frequency of magnetic resonance the thickness of the superstrate is only $\lambda/12$.

B. Impedance matrix representation

Based on the analysis for normally incident plane waves we derive an impedance matrix representation [53] connecting the

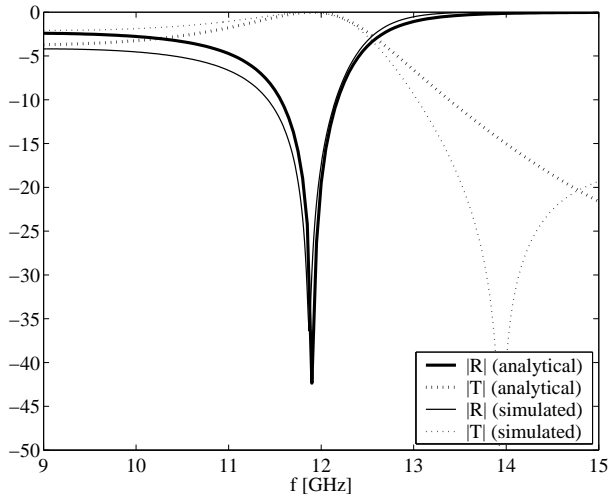


Fig. 2. Calculated and simulated reflection and transmission coefficients for two grids of capacitively loaded wires.

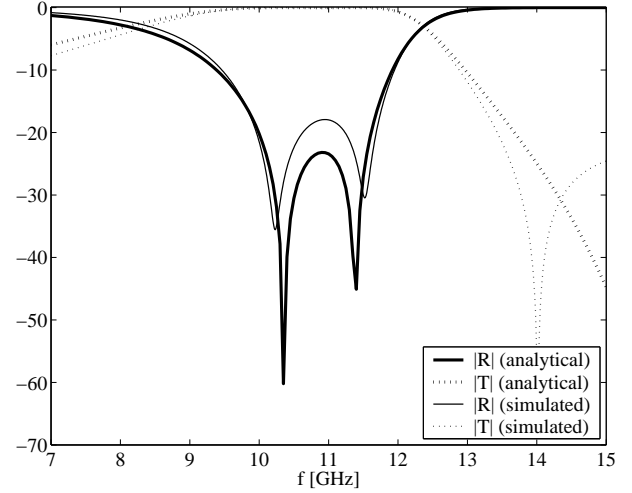


Fig. 3. Calculated and simulated reflection and transmission coefficients for two grids of capacitively loaded wires with one grid of continuous wires in between them.

total (averaged) electric field in the grid planes to the averaged current densities flowing in the grids:

$$\begin{pmatrix} \widehat{E}_1^{\text{tot}} \\ \widehat{E}_2^{\text{tot}} \\ \widehat{E}_3^{\text{tot}} \end{pmatrix} = \begin{pmatrix} Z_{11} & Z_{12} & Z_{13} \\ Z_{21} & Z_{22} & Z_{23} \\ Z_{31} & Z_{32} & Z_{33} \end{pmatrix} \begin{pmatrix} \widehat{J}_1 \\ \widehat{J}_2 \\ \widehat{J}_3 \end{pmatrix}. \quad (20)$$

This representation is derived to enable later the construction of an equivalent superstrate circuit model taking into account the mutual interaction between the grids. For illustration purposes let us conduct the derivation in details for the first grid. Using the impedance matrix notation the total field in the plane of this grid reads

$$\widehat{E}_1^{\text{tot}} = Z_{11}\widehat{J}_1 + Z_{12}\widehat{J}_2 + Z_{13}\widehat{J}_3. \quad (21)$$

Following the definition of the impedance matrix [53] Z_{11} is the total electric field in the first grid plane divided by the averaged current flowing in that grid, assuming that currents in

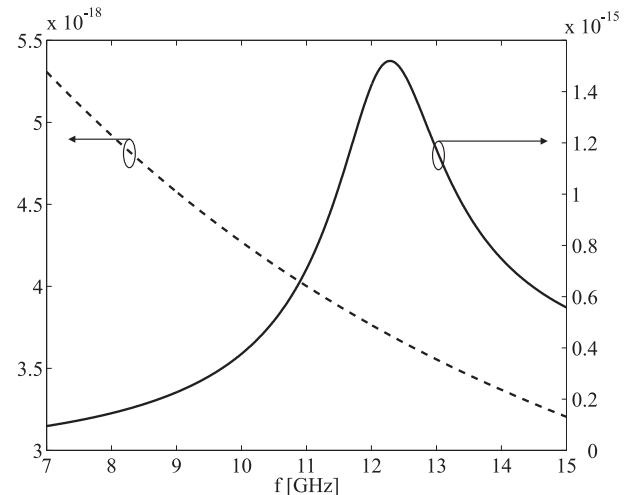


Fig. 4. Densities of induced electric (dashed line) and magnetic (solid line) dipole moments. The superstrate consists of two grids of capacitively loaded wires.

the other grids are zero. The component of the total (averaged) electric field parallel to the grids, defined in the plane of grid i is by definition [46]

$$\widehat{E}_i^{\text{tot}} = E^{\text{ext}} + E_i^{\text{sc}} = E^{\text{ext}} - \frac{\eta}{2} \widehat{J}_i. \quad (22)$$

When we solve E^{ext} from (5) (now $I_2 = I_3 = 0$) and substitute the result in (22), the following expression is obtained:

$$\widehat{E}_1^{\text{tot}} \Big|_{I_2=I_3=0} = -d \left(\beta(0) - \alpha^{-1} + \frac{\eta}{2d} \right) \widehat{J}_1 = Z_{11} \widehat{J}_1. \quad (23)$$

Next, consider the definition of Z_{12} . The plane-wave term disappears in (22) since now the current flowing in the first grid is by definition zero [53]. Thus, we get (after we solve E^{ext} from (5) assuming that $I_1 = I_3 = 0$):

$$\widehat{E}_1^{\text{tot}} \Big|_{I_1=I_3=0} = -d\beta(h) \widehat{J}_2 = Z_{12} \widehat{J}_2. \quad (24)$$

Similarly for Z_{13} :

$$\widehat{E}_1^{\text{tot}} \Big|_{I_1=I_2=0} = -d\beta(2h) \widehat{J}_3 = Z_{13} \widehat{J}_3. \quad (25)$$

After repeating the above procedure for the second and third grid we get the following expressions for the impedances:

$$Z_{11} = Z_{33} = -d \left(\beta(0) - \alpha^{-1} + \frac{\eta}{2d} \right), \quad (26)$$

$$Z_{22} = -d \left(\beta(0) - \alpha_0^{-1} + \frac{\eta}{2d} \right), \quad (27)$$

$$Z_{21} = Z_{12} = Z_{32} = Z_{23} = -d\beta(h), \quad (28)$$

$$Z_{13} = Z_{31} = -d\beta(2h). \quad (29)$$

C. Equivalent circuit representation

The equivalent circuit of the superstrate can be derived by looking at the actual structure shown in Fig. 1. The resulting circuit is shown in Fig. 5. Let us clarify the reasoning behind the circuit in details: In Fig. 5 L denotes the averaged (quasi-static) inductance of a wire array which is available e.g. in [42]. C is the capacitance of a short strip (formula for this estimation is available e.g. in [46]) and C_0 is the capacitance between the metal strips in the grid plane. Essentially the series connection of L and C_0 models the capacitively loaded wire medium [35] and we have added C in parallel to this connection to represent the resonance due to strip length (this effect is rather weak in the quasi-static regime). Further, C_1 and C_2 are the capacitance between the dipole grid and wire grid, and the capacitance between the dipole grids, respectively. Textbook formulas have been used to estimate C_0, C_1, C_2 . M_2 and M_3 are the mutual inductances representing the interaction between different grids. These are obtained as the quasi-static limit for $\text{Im}\{Z_{21}\}$ and $\text{Im}\{Z_{31}\}$, respectively:

$$-M_2 = \frac{\mu_0}{2} \left(-h - \frac{d}{\pi} \log |1 - e^{-2\pi h/d}| \right), \quad (30)$$

$$-M_3 = \frac{\mu_0}{2} \left(-2h - \frac{d}{\pi} \log |1 - e^{-4\pi h/d}| \right). \quad (31)$$

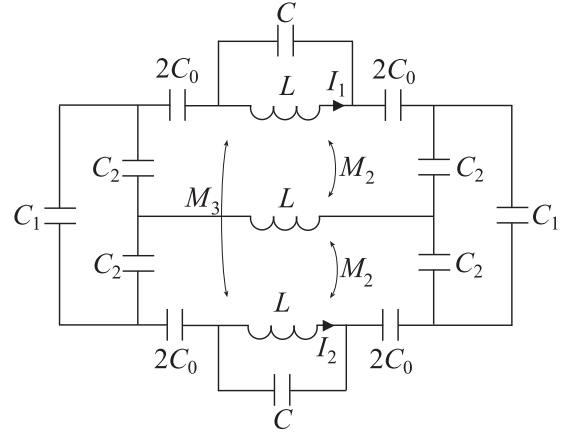


Fig. 5. Equivalent circuit model for the three grid superstrate shown in Fig. 1a.

The equivalent circuit representation allows us to quickly determine the eigen modes of the superstrate. As an example of its use we choose once again the structure consisting only of capacitively loaded wires, and calculate using nodal analysis the frequency at which the currents induced to the grids (currents I_1 and I_2 in Fig. 5) are equal in amplitude and out of phase. This frequency roughly corresponds to the deep minimum of the reflection coefficient at 11.9 GHz observed in Fig. 3. The analysis based on the equivalent circuit predicts that the currents have equal amplitude and opposite phase at frequency 10.2 GHz. This result slightly differs from the result predicted by the electrodynamic model (the difference is approximately 15 %), however, when taking into account all the limitations of the equivalent circuit representation (quasi-static nature) the agreement between the results is considered reasonably good.

IV. FINITE SIZE SUPERSTRATES ILLUMINATED BY WIRE ANTENNAS

In this section we study and discuss the performance of finite size superstrates when illuminated by real antennas. Our primary source is a resonant $\lambda/2$ -dipole antenna, and we consider here for the sake of clarity only the superstrate consisting of two grids of capacitively loaded wires. The antenna geometry is depicted schematically in Fig. 6. The antenna could also be backed by a ground plane, and the superstrate could be used as a tool to create Fabry-Perot resonant cavity to possibly further enhance the directivity. This design option is not, however, considered here. The number of wires in x -direction is N_x and in this analysis we call

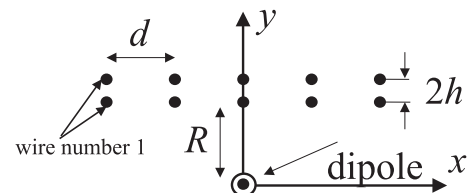


Fig. 6. Schematic illustration of the antenna geometry. The black dots denote capacitively loaded wires. Number of wires in x -direction is N_x .

the grid closest to the dipole “grid 1”. The distance between the grids $R = 2h$, and the distance between the wires in the grids d is the same as introduced in Section III. Compared to the numerical validation presented at the end of Section III (in that case we wanted the modeled setup to correspond as accurately as possible to the structure considered in [34]) we make some changes to the structural parameters of the loaded wires. The distributed capacitance level is, however, kept at the same value as considered in Section III to ease the comparison. We do the modifications in order to assure that the metal strips are electrically short enough so that the model based on capacitively loaded wires remains accurate. The modified parameters read (see Fig. 1): $l_d = 5.74$ mm, $l = l_d + 0.1$ mm, $t = 1.25$ mm.

The radiation characteristics (radiation patterns and the radiation resistance) of the antenna structure are analytically calculated using the method introduced in [54], [55]. This method is explicit and accurate [54], and it is based on the rigorous summation of the fields created by the source currents and currents induced to the passive wires. The method assumes that the wires are long (the propagation constant in the z -direction is the same for all the wires), but it allows us to conveniently study separately the currents induced to the passive wires by each of the source harmonics. At the end of this section we verify the radiation characteristics of the final antenna design (having finite wire height) using a commercial method-of-moments solver FEKO [56].

A. Example results

Inevitably there will be a strong near field interaction between the dipole and the grids when R is moderate. Compared to the situation analyzed in Section III (the number of wires is infinite in x -direction) the finite number of wires (in practise also the finite height of wires) leads to the formation of standing waves along x -direction. This formation also strongly depends on the location of the source and on the number of wires. It was also observed in [8] that the radiation resistance of antennas using capacitively loaded wires as beam shapers can change rather strongly as a function of frequency. Thus, the practical antenna design² based on the proposed superstrates will be a detailed optimization problem, and this is out of the scope of the present paper. Here we only illustrate some of the main observations presented so far in the paper. At the end of the section an antenna structure showing acceptable performance will be designed.

Our preliminary calculations have shown that when the dipole is positioned rather close to the grid (in our first calculations $R = 2h$) the frequency at which the currents in the grids cancel each other is located in the vicinity of 12.8 GHz. This frequency is roughly 7 % higher than the corresponding frequency observed using plane wave excitation, and the slight difference can well be explained by the above discussion. As an example demonstrating the cancelation of currents we choose $N_x = 15$, $R = 2h$ and calculate the amplitudes

²In practise measures such as the impedance bandwidth, deviation in beam widths, backward radiation level, and side lobe levels as a function of frequency, should be analyzed in details.

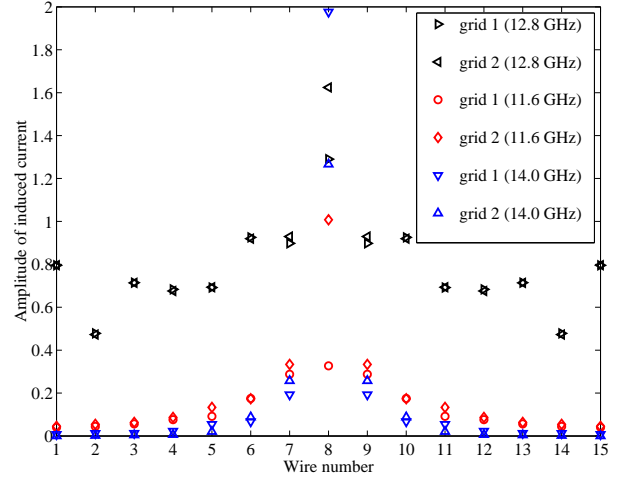


Fig. 7. Amplitudes of currents induced to the wires at different frequencies. The numbering of wires starts from the leftmost wire in the grid, see Fig. 6.

of currents induced to the grids by the source harmonic corresponding to $k_z = 0$ (the amplitude of the feed current is assumed to be unity). The phase difference between the currents induced to the pairing wires will also be calculated. We perform the calculation at three frequencies: At 12.8 GHz (corresponding to the expected transmission frequency), at 11.6 GHz, and at 14.0 GHz. The amplitudes of currents induced to the grids at different frequencies are depicted in Fig. 7. The phase differences in the pairing wires are shown in Fig. 8.

When inspecting the amplitude levels we observe that at 12.8 GHz the amplitudes of the induced current are most uniformly distributed in the grids. At the lower and higher example frequency only the wires closest to the dipole are strongly excited. We also notice that at 12.8 GHz the phase difference in all the wires is very close to π implying that the currents in the grids cancel each other allowing the particular harmonic to propagate through the grid. At 11.6 GHz the phase difference is close to π in most of the pairing wires

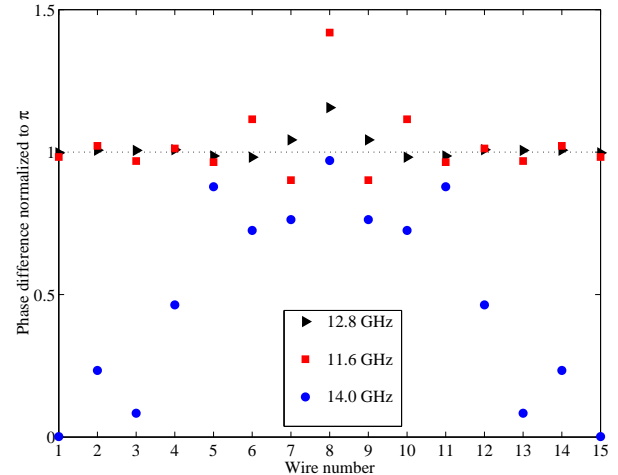


Fig. 8. Phase differences in the pairing wires at different frequencies. The phase difference has been normalized to π .

but only the wires closest to the dipole are effectively excited (please see the amplitude levels). At 14.0 GHz the phase difference deviates in several pairing wires significantly from π . It was observed in [55] that when a wire antenna is placed very close to a lattice of (properly) capacitively loaded wires the source current and the current induced to the closet passive wires add up constructively leading to reasonable high radiation resistance. The radiation resistance, calculated as in [54], is at the three studied frequencies 71.6 Ω , 43.5 Ω , and 9.6 Ω , respectively. Thus, at 12.8 GHz the structure radiates effectively and can be easily matched to a standard 75 Ω feeding line.

Though the finite size superstrate performs with a realistic primary source as discussed in the previous sections (in the vicinity of 12.8 GHz) and the radiation resistance has a reasonably high value, the radiation pattern, depicted in Fig. 9, is not suitable for most of the applications. With the particular structural parameters the phase difference between different pairing currents is favorable for multiple side lobes to appear in the H-plane. The optimization of this particular structure to perform in a desirable way would be, as mentioned earlier, an optimization problem and out of the scope of this paper. Below we will, however, present a design that performs in a relatively desirable manner.

We reduce the number of wires in x -direction to $N_x = 5$ (the width of the superstrate is approximately 1.2λ at 12.8 GHz) and change the distance between the source and the first grid to $R = 4h$. The calculated radiation patterns, and the H-plane radiation pattern simulated in FEKO are shown in Fig. 10. They are in very good agreement showing the feasibility of the used analytical method. The wire height in FEKO simulations is 3λ . The calculated radiation resistance is 55.8 Ω implying that the structure radiates effectively and is easy to match to a 50 Ω feeding line. The directivity obtained

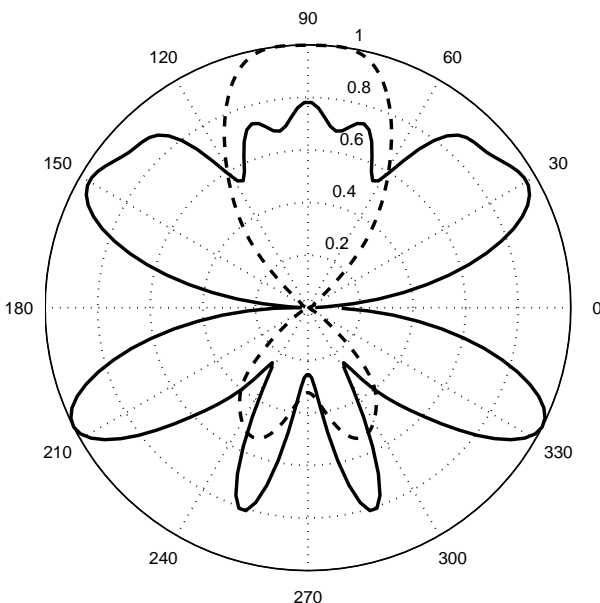


Fig. 9. Normalized radiation patterns at 12.8 GHz for the antenna structure with $N_x = 15$, $R = 2h$. Solid line corresponds to H-plane, dashed line corresponds to E-plane.

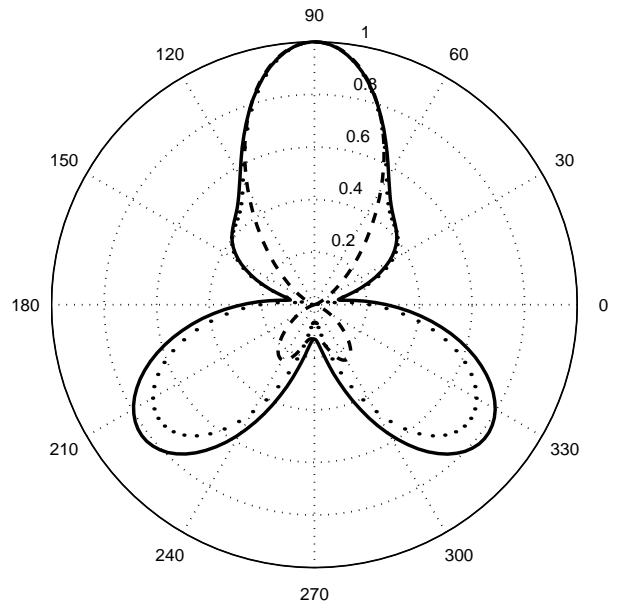


Fig. 10. Normalized radiation patterns at 12.8 GHz for the antenna structure with $N_x = 5$, $R = 4h$. Solid line corresponds to H-plane, dashed line corresponds to E-plane. The dotted result is the simulated (FEKO) H-plane radiation pattern.

from the simulations is 6.4 dBi at 12.8 GHz, and the total thickness of the antenna structure is approximately $\lambda/3.7$ at 12.8 GHz.

V. CONCLUSION

We have presented a method to analyze the characteristics of a class of antenna superstrates based on periodical grids of loaded wires. In addition to this, the physics behind the radiation mechanism of such superstrates has been clarified. Local field method has been used to solve for the currents induced to the superstrates by incident plane-wave field, and reflection and transmission properties of the superstrates have been studied. The analytical results have been verified using numerical simulations. In addition to this, we have derived an impedance matrix and equivalent circuit representations for the superstrates. As a practical application we have considered finite size superstrates illuminated by realistic sources, and discussed the effects of finite structural dimensions to the superstrate performance. We believe that the results presented here can be helpful to later design optimized antennas utilizing the proposed superstrates.

ACKNOWLEDGEMENT

One of the authors (P.M.T. I.) wishes to thank Dr. Pavel A. Belov for useful discussions related to the wire media modeling.

REFERENCES

- [1] W. E. Kock, "Metal-lens antennas," *Proc. IRE*, vol. 34, pp. 828–836, 1946.
- [2] —, "Metallic delay lenses," *Bell System Technical J.*, vol. 27, pp. 58–82, 1948.

- [3] J. B. Brown, "Artificial dielectrics," in *Progress in Dielectrics*, 2nd ed., J. B. Birks and J. H. Schulman, Eds. London: Heywood Co. Ltd., 1960, pp. 193-225.
- [4] W. Rotman, "Plasma simulation by artificial dielectrics and parallel plate media," *IRE Trans. Antennas Propag.*, vol. 10, pp. 82-95, 1962.
- [5] K. E. Golden, "Plasma simulation with an artificial dielectric in a horn geometry," *IEEE Trans. Antennas Propag.*, vol. 13, no. 4, pp. 587-594, 1965.
- [6] I. J. Bahl and K. C. Gupta, "A leaky-wave antenna using an artificial dielectric medium," *IEEE Trans. Antennas Propag.*, vol. 22, no. 1, pp. 119-122, 1974.
- [7] P. Ikonen, C. Simovski, and S. Tretyakov, "Compact directive antennas with a wire-medium artificial lens," *Microwave Opt. Technol. Lett.*, vol. 43, no. 6, pp. 467-469, 2004.
- [8] P. Ikonen, M. Kärkkäinen, C. Simovski, P. Belov, and S. Tretyakov, "Light-weight base station antenna with artificial wire-medium lens," *IEE Proc. Microwaves, Antennas and Propag.*, vol. 153, no. 2, pp. 163-170, 2006.
- [9] B. Gralak, S. Enoch, and G. Tayeb, "Anomalous refractive properties of photonic crystals," *J. Opt. Soc. Am. B*, vol. 17, no. 6, pp. 1012-1020, 2000.
- [10] M. Notomi, "Theory of light propagation in strongly modulated photonic crystals: Refractionlike behavior in the vicinity of the photonic band gap," *Phys. Rev. B*, vol. 62, no. 16, pp. 10696-10705, 2000.
- [11] B. T. Schwartz and R. Piestun, "Total external reflection from metamaterials with ultralow refractive index," *J. Opt. Soc. Am. B*, vol. 20, no. 12, pp. 2448-2453, 2003.
- [12] S. Enoch, G. Tayeb, P. Sabouroux, N. Guérin, and P. Vincent, "A metamaterial for directive emission," *Phys. Rev. Lett.*, vol. 89, no. 21, 2139021, 2002.
- [13] S. Enoch, G. Tayeb, and B. Gralak, "The richness of the dispersion relation of electromagnetic band-gap materials," *IEEE Trans. Antennas Propag.*, vol. 51, no. 10, pp. 2659-2666, 2003.
- [14] G. Lovat, P. Burghignoli, F. Capolino, D. R. Jackson, and D. R. Wilton, "Analysis of directive radiation from a line source in a metamaterial slab with low permittivity," *IEEE Trans. Antennas Propag.*, vol. 54, no. 3, pp. 1017-1030, 2006.
- [15] G. Tayeb and D. Maestre, "Rigorous theoretical study of finite-size two-dimensional photonic crystals doped by microcavities," *J. Optical Soc. America A*, vol. 14, no. 12, pp. 3323-3332, 1997.
- [16] M. Thévenot, C. Cheype, A. Reineix, and B. Jecko, "Directive photonic-bandgap antennas," *IEEE Trans. Microwave Theory Tech.*, vol. 47, no. 11, pp. 2115-2122, 1999.
- [17] B. Temelkuran, M. Bayindir, E. Ozbay, R. Biswas, M. M. Sigalas, G. Tuttle, and K.-M. Ho, "Photonic crystal-based resonant antenna with a very high directivity," *J. Appl. Phys.*, vol. 87, no. 1, pp. 603-605, 2000.
- [18] R. Biswas, E. Ozbay, B. Temelkuran, M. Bayindir, M. M. Sigalas, and K.-M. Ho, "Exceptionally directional sources with photonic-bandgap crystals," *J. Opt. Soc. Am. B*, vol. 18, no. 11, pp. 1684-1688, 2001.
- [19] C. Cheype, C. Serier, M. Thévenot, T. Monédière, A. Reineix, and B. Jecko, "An electromagnetic bandgap resonator antenna," *IEEE Trans. Antennas Propag.*, vol. 50, no. 9, pp. 1285-1290, 2002.
- [20] T. Akalin, J. Danglot, O. Vanbésien, and D. Lippens, "A highly directive dipole antenna embedded in a Fabry-Perot type cavity," *IEEE Microw. Wireless Comp. Lett.*, vol. 12, no. 2, pp. 48-50, 2002.
- [21] Y. J. Lee, J. Yeo, R. Mittra, and W. S. Park, "Application of electromagnetic bandgap (EBG) superstrates with controllable defects for a class of patch antennas as spatial angular filters," *IEEE Trans. Antennas Propag.*, vol. 53, no. 1, pp. 224-235, 2005.
- [22] G. von Trentini, "Partially reflecting sheet arrays," *IRE Trans. Antennas Propag.*, vol. 4, pp. 666-671, 1956.
- [23] A. P. Feresidis and J. C. Vardaxoglou, "High gain planar antenna using optimized partially reflective surfaces," *IEE Proc. Microwaves, Antennas and Propag.*, vol. 148, no. 6, pp. 345-350, 2001.
- [24] G. K. Palikaras, A. P. Feresidis, and J. C. Vardaxoglou, "Cylindrical electromagnetic bandgap structures for directive base station antennas," *IEEE Antennas Wireless Propag. Lett.*, vol. 3, pp. 87-89, 2004.
- [25] A. P. Feresidis, G. Goussetis, S. Wang, and J. C. Vardaxoglou, "Artificial magnetic conductor surfaces and their application to low-profile high-gain planar antennas," *IEEE Trans. Antennas Propag.*, vol. 53, no. 1, pp. 209-215, 2005.
- [26] S. Wang, A. P. Feresidis, G. Goussetis, and J. C. Vardaxoglou, "High-gain subwavelength resonant cavity antennas based on metamaterial ground planes," *IEE Proc. Microwaves, Antennas and Propag.*, vol. 153, no. 1, pp. 1-6, 2006.
- [27] H. Boutayeb and T. A. Denidni, "Analysis and design of a high-gain antenna based on metallic crystals," *J. Electromagn. Waves and Appl.*, vol. 20, no. 5, pp. 599-614, 2006.
- [28] Y. J. Lee, J. Yeo, R. Mittra, and W. S. Park, "Design of a high-directivity electromagnetic band gap (EBG) resonator antenna using a frequency-selective surface (FSS) superstrate," *Microwave Opt. Technol. Lett.*, vol. 43, no. 6, pp. 462-467, 2004.
- [29] N. G. Alexopoulos and D. R. Jackson, "Fundamental superstrate (cover) effects on printed circuit antennas," *IEEE Trans. Antennas Propag.*, vol. AP-32, no. 8, pp. 807-816, 1984.
- [30] D. R. Jackson and N. G. Alexopoulos, "Gain enhancement methods for printed circuit antennas," *IEEE Trans. Antennas Propag.*, vol. AP-33, no. 9, pp. 976-987, 1985.
- [31] D. R. Smith, W. J. Padilla, D. C. Vier, S. C. Nemat-Nasser, and S. Schultz, "Composite medium with simultaneously negative permeability and permittivity," *Phys. Rev. Lett.*, vol. 84, no. 18, pp. 4184-4187, 2000.
- [32] R. W. Ziolkowski and A. D. Kipple, "Application of double negative materials to increase the power radiated by electrically small antennas," *IEEE Trans. Antennas Propag.*, vol. 51, no. 10, pp. 2626-2640, 2003.
- [33] B.-I. Wu, W. Wang, J. Pacheco, X. Chen, J. Lu, T. M. Grzegorzczak, J. A. Kong, P. Kao, P. A. Theophilakos, M. J. Hogan, "Anisotropic metamaterials as antenna substrate to enhance directivity," *Microwave Opt. Technol. Lett.*, vol. 48, no. 4, pp. 680-683, 2006.
- [34] E. Saenz, R. Gonzalo, I. Ederra, and P. de Maagt, "Design of a planar meta-surface based on dipoles and wires for antenna applications," in *Proc. EuCAP 2006*, Nice, France, Nov. 6-10, 2006, paper 349401.
- [35] P. A. Belov, C. R. Simovski, S. A. Tretyakov, "Two-dimensional electromagnetic crystals formed by reactively loaded wires," *Phys. Rev. E*, vol. 66, 036610, 2002.
- [36] D. Lockyer, C. Moore, R. Seager, R. Simpkin, and J. C. Vardaxoglou, "Coupled dipole arrays as reconfigurable frequency selective surfaces," *Electron. Lett.*, vol. 30, no. 16, pp. 1258-1259, 1994.
- [37] J. C. Vardaxoglou and D. Lockyer, "Modified FSS response from two sided and closely coupled arrays," *Electron. Lett.*, vol. 30, no. 22, pp. 1818-1819, 1994.
- [38] A. P. Feresidis, G. Apostolopoulos, N. Serfas, and J. C. Vardaxoglou, "Closely coupled metalodielectric electromagnetic band-gap structures formed by double-layer dipole and tripole arrays," *IEEE Trans. Antennas and Propag.*, vol. 52, no. 5, pp. 1149-1158, 2004.
- [39] J. B. Pendry, A. J. Holden, D. J. Robbins, and W. J. Stewart, "Magnetism from conductors and enhanced nonlinear phenomena," *IEEE Trans. Microwave Theory Tech.*, vol. 47, no. 11, pp. 2075-2084, 1999.
- [40] G. Dolling, C. Enkrich, M. Wegener, J. F. Zhou, C. M. Soukoulis, and S. Linden, "Cut-wire pairs and plate pairs as magnetic atoms for optical metamaterials," *Opt. Lett.*, vol. 30, no. 23, pp. 3198-3200, 2005.
- [41] P. A. Belov, S. A. Tretyakov, A. J. Viitanen, "Dispersion and reflection properties of artificial media formed by regular lattices of ideally conducting wires," *J. Electromagn. Waves and Appl.*, vol. 16, no. 8, pp. 1153-1170, 2002.
- [42] S. I. Maslovski, S. A. Tretyakov, and P. A. Belov, "Wire media with negative effective permittivity: A quasi-static model," *Microwave Opt. Technol. Lett.*, vol. 35, no. 1, pp. 47-51, 2002.
- [43] V. M. Shalaev, W. Cai, U. K. Chettiar, H.-K. Yuan, A. K. Sarychev, V. P. Drachev, and A. V. Kildishev, "Negative index of refraction in optical metamaterials," *Optics Lett.*, vol. 30, no. 24, pp. 3356-3358, 2005.
- [44] J. Zhou, L. Zhang, G. Tuttle, T. Koschny, and C. Soukoulis, "Negative index materials using simple short wire pairs," *Phys. Rev. E*, vol. 73, p. 041101, 2006.
- [45] L. B. Felsen and N. Marcuvitz, *Radiation and scattering of waves*, Piscataway, NJ: IEEE Press, 1994.
- [46] S. Tretyakov, *Analytical modeling in applied electromagnetics*, Norwood, MA: Artech House, 2003.
- [47] V. V. Yatsenko, S. A. Tretyakov, S. I. Maslovski, A. A. Sochava, "Higher order impedance boundary conditions for sparse wire grids," *IEEE Trans. Antennas Propag.*, vol. 48, no. 5, pp. 720-727, 2000.
- [48] J. D. Jackson, *Classical electrodynamics*, 3rd ed., New York: John Wiley & Sons, 1999.
- [49] S. I. Maslovski and S. A. Tretyakov, "Full-wave interaction field in two-dimensional arrays of dipole scatterers," *Int. J. Electron. Commun. (AEU)*, vol. 53, no. 3, pp. 135-139, 1999.
- [50] V. V. Yatsenko, S. I. Maslovski, and S. A. Tretyakov, "Electromagnetic interaction of parallel arrays of dipole scatterers," in *Progress in Electromagnetics Research: PIER* vol. 25, pp. 285-307, 2000.

- [51] V. V. Yatsenko, S. I. Maslovski, S. A. Tretyakov, S. L. Prosvirnin, and S. Zouhdi, "Plane-wave reflection from double arrays of small magnetoelectric scatterers," *IEEE Trans. Antennas Propag.*, vol. 51, no. 1, pp. 2–11, 2003.
- [52] The www-page of Ansoft, <http://www.ansoft.com>.
- [53] D. M. Pozar, *Microwave engineering*, 2nd Ed., New York: John Wiley & Sons, 1998.
- [54] S. He, C. R. Simovski, and M. Popov "An explicit and efficient method for obtaining the radiation characteristics of wire antennas in metallic photonic bandgap structures," *Microwave Opt. Techn. Lett.*, vol. 26, no. 2, pp. 67–73, 2000.
- [55] C. R. Simovski and S. He, "Antennas based on modified metallic photonic bandgap structures consisting of capacitively loaded wires," *Microwave Opt. Technol. Lett.*, vol. 31, no. 3, pp. 214–221, 2001.
- [56] The www-page of FEKO, <http://www.feko.info>.